UNITED STATES DEPARTMENT OF THE INTERIOR

GEOLOGICAL SURVEY

SEISMIC EVIDENCE FOR AN EXTENSIVE GAS-BEARING LAYER AT SHALLOW DEPTH, OFFSHORE FROM PRUDHOE BAY, ALASKA

By

Gary Boucher, Erk Reimnitz, and Ed Kempema

Open-file report 80- 809

1980

SEISMIC EVIDENCE FOR AN EXTENSIVE GAS-BEARING LAYER AT SHALLOW DEPTH, OFFSHORE FROM PRUDHOE BAY, ALASKA

Gary Boucher, Erk Reimnitz, and Ed Kempema

ABSTRACT

High resolution seismic reflection data recorded offshore from Prudhoe Bay, Alaska, were processed digitally to determine the reflectivity structure of the uppermost layers of the seafloor. A prominent reflector found at 27 m below the mudline (water depths 7-9 m) has a negative reflection coefficient greater than 0.5. The large acoustic impedance contrast, coupled with a report of gas encountered at a corresponding depth in a nearby drillhole, shows that the reflector is the upper boundary of a zone containing gas. The gas exists in sandy gravel capped by stiff, silty clay. Analysis of unprocessed conventional high-resolution records from the region indicates that the gas-bearing layer may extend over an area of at least 50 km^2 at depths of 19-35 m below the mudline. Similar-appearing reflectors, previously unexplained, occur in patches over wide regions of the shelf where offshore oil development is beginning at a rapid pace. This suggests the exercise of caution with respect to possible hazards from shallow gas pockets.

INTRODUCTION

During August 1979, the authors tape-recorded high-resolution seismic reflection data offshore from Prudhoe Bay, Alaska. Our purpose was to apply vertical seismic reflection techniques, with digital processing, to the mapping and characterization of ice-bonded material in the offshore environment near Prudhoe Bay. An unexpected result of that study is the identification of a strong reflector at depths between 19 and 35 m below the mudline as the upper boundary of a gas-bearing layer. The identification is supported by evidence from a nearby geotechnical borehole. In this paper, we discuss

the seismic processing used, and we extend the results to other seismic records from the same general area. Our study shows that the gas-bearing layer underlies an area of at least 50 km^2. We discuss some implications of these results relative to offshore development in the area.

GEOLOGIC SETTING

During February and March 1979, 20 geotechnical boreholes were drilled and cored on Federal tracts within the Beaufort Sea lease sale area (Harding-Lawson Assoc., 1979). The maximum depths of the boreholes were between 24.8 and 91.8 m below the mudline. In the course of collecting seismic profiles across a number of these drill holes, we noticed an anomalously strong sub-bottom reflector in the vicinity of a drill hole at $70^{o}23.012'$N, $147^{o}41.003'$ W (Hole 11 of Harding-Lawson Assoc., 1979).

The drilling log for hole no. 11 indicates an upper layer of predominantly silty sand 3 m thick, underlain by a stiff or very stiff silt with thin layers of organic material and fine sand. Below 17 m, possible thin ice lenses were observed, and below 24 m the material was ice-bonded. Around 25 m below the mudline, a layer of sandy gravel was penetrated, containing occasional lenses of ice-bonded sand. While drilling in this sandy gravel, flammable gas was observed bubbling out of the drilling mud. The hole therefore was terminated at 29 m depth. This depth corresponds to that of the strong seismic reflector.

METHODS

Seismic evidence for the existence of ice-bonded sediment (permafrost) in offshore areas of the Beaufort sea in the past has been derived mainly from seismic refraction studies (Hunter and others, 1978, and Rogers and Morack, 1978, for example). However, seismic reflection methods should provide better horizontal resolution and a more complete description of vertical

geometry. In order to use seismic reflection methods to identify ice-bonded or gas-bearing sediments on the basis of measurable physical properties, one must derive reflection coefficients from the amplitudes of reflection events.

However, most seismic sources do not produce a simple waveform, which is easily measured in the presence of multiple, closely spaced reflectors and noise. Thus, deconvolution is required as an intermediate step to convert each seismic reflection event in the signal to a waveform of minimum duration whose amplitude and polarity can be easily measured. Berkhout (1977) explains why a zero-phase wavelet is the optimum waveform for making such measurements. Furthermore, the width of the wavelet will be a minimum if the amplitude spectrum of the seismic pulse is smooth and broad. In this study, zero-phase wavelet deconvolution was performed by constructing an explicit model of the seismic source pulse based on the direct (water-wave) arrival, which we deliberately recorded. This model for the seismic source pulse was then cross-correlated with the seismic trace and inverse filtered to achieve the optimum seismic trace for making measurements. The use of cross-correlation in this way to achieve a zero-phase wavelet, and the digital filtering involved are explained in books on digital processing, such as that by Gold and Rader (1969). Because of the limited signal bandwidth of the final output seismic trace, the seismic wavelet is not a single spike, but is like a W-shape with small negative excursions, as shown in fig. 1. The wavelet's polarity is unambiguous so long as the signal-to-noise ratio is sufficiently large.

Seismic reflection data were recorded on analog magnetic tape using a Uniboom source aboard the R/V KARLUK. We digitized the data at a rate of 10,000 samples per second for computer processing, and performed zero-phase wavelet deconvolution as explained above. The limits of useful signal frequency range were 150 and 2000 Hz. The full width of the deconvolved seismic pulse was about 0.8 msec, corresponding to a vertical resolution of about 0.6 m at the speed of sound in water.

ANALYSIS

Figure 2 shows the shipboard seismic record, and delineates the small area chosen for detailed digital analysis. Since the record is of rather poor quality, we show a reprocessed section in figure 3. The prominent reflector at about 38 msec is labeled as the "gas" reflector, and its first water-column multiple reflection can be seen about 13 msec below. The records in figures 2 and 3 have been subjected to automatic gain control, but the reflector of interest nevertheless appears strong. In order to quantify the strength of the reflector and determine its polarity, the seismic section was deconvolved and plotted as shown in figure 4. On the left side of figure 2, the deconvolved seismic record section is shown. On the right side of figure 4, the full-amplitude wiggle-traces are shown for the same data subjected to 5-fold vertical stacking. Here the relative strength and reversed polarity of the prominent reflector are apparent in comparison with the reflection from the water-sediment interface. To permit quantitative measurements of the reflection coefficient of the prominent reflector, the data were presented as in figure 5. after 20-fold vertical stacking to further reduce random noise. We do not know the amplitude of the outgoing seismic pulse, and the amplitude of the seafloor multiple is too small to measure accurately. Therefore we cannot measure reflection coefficients directly. However, given a reasonable reflection coefficient of at least 0.2 (Hamilton, 1969) for the silty sand at the seafloor, we can estimate the reflection coefficient of the strong subbottom reflector. We compare the amplitude of the seafloor reflection with that of the subbottom reflector, and allow for a return path across several interfaces, including the seafloor. We conclude that the magnitude of the reflection coefficient of the gas reflector cannot be less than 0.5. The implications of a reflection coefficient this large become clear from the following considerations. The simplest approximation for the reflection coefficient, the Rayleigh plane-wave reflection coefficient (Dobrin, 1960, p. 25) is given by

$$R = \frac{\rho_2 v_2 - \rho_1 v_1}{\rho_2 v_2 + \rho_1 v_1}$$, where

R is the amplitude ratio between the incident and reflected plane waves at normal incidence on an interface, ρ_1 is the bulk density of the upper medium ρ_2 is the bulk density of the lower medium, and v_1 and v_2 are the sound velocities in the upper and lower media, respectively. If the acoustic impedance, $\rho_2 v_2$, of the lower medium is less than that of the upper medium, the reflection coefficient will be negative and the reflection will be inverted. The physical problem is to achieve the contrast between $\rho_1 v_1$ and $\rho_2 v_2$ needed to explain reflection coefficient observations, given the materials known to be present.

We demonstrate the presence of gas in the reflecting layer by showing that, even with the most unfavorable assumptions for the product $\rho_1 v_1$, the required value of $\rho_2 v_2$ is too small to be explained without significant amounts of gas in the sediment pore space. Taking R = 0.5 (a minimum), ρ_1 = 1.8 g/cm^3, v_1 = 3000 msec, and solving for the required value of $\rho_2 v_2$, gives $\rho_2 v_2 = 1.8 \times 10^5$ g cm^{-2} sec^{-1}, probably an over estimate. This is far too low for the sandy gravel, probably frozen, known from the drill log to be present, without interstitial gas. Therefore, a significant quantity of gas must be present in the pore space of the material underlying the reflecting interface, serving to reduce both bulk density and compressional velocity enough to achieve the observed low value of acoustic impedance, $\rho_2 v_2$. The report of bubbling gas from the drilling log is supporting evidence.

A constraint on the minimum thickness of the gas-bearing layer is a rule of thumb that a layer must be at least 1/5 of a wavelength thick to yield a substantial reflection at a given signal frequency. In view of the strength of the reflector that is observed, it is more likely to be at least one-half

wavelength thick. Since we commonly observe a strong reflection with signals peaking near 1200 Hz, we may conservatively state that the layer, where it is strongly reflecting, is at least 1 m thick. Figure 6 shows a magnified view of a portion of figure 4. There is an indication of a positive reflector about 1.5 m below the gas reflector, which appears to pinch out further to the right. If this lower reflector represents the bottom of the gas zone, then the gas zone may be a bit more than a meter thick. Otherwise we have no constraint on the maximum thickness of the gas zone.

The digital seismic analysis was performed for a location about 600 m from drill hole no. 11. However, the prominent seismic reflector can be traced to the location of the drill hole without interruption, and maintains its character. Therefore we are confident that the seismic data are correctly correlated with the borehole data.

The characteristic seismic reflector identified as gas can be traced on conventional high-resolution seismic records from the surrounding area, obtained during several years of seismic profiling. On these records (see figure 7), the reflector is recognized on the basis of (1) its strength (bearing in mind that most of such records were made with automatic gain control), (2) its negative polarity (sometimes ambiguous), (3) its continuity over long distances, and (4) its restriction to a narrow range of subbottom depths. In some areas the characteristic reflector appears weaker, but nevertheless prominent. The apparently diminished reflection amplitude may result from a change in some property of the reflecting layer, from a change in the overlying sediments, or from the presence of boulders on the seafloor. Figure 8 shows the seismic trackline coverage available in the study area, and the areal extent of the gas-bearing layer mapped by use of the seismic record as either strong or weak.

Figure 8 also shows the depth of the gas-bearing layer beneath the mudline. One characteristic feature of the gas-charged seismic reflector is its abrupt, unexplained termination in many areas. Where such terminations occur, figure 8 shows the boundary of the gas patch as a solid line. Where the reflector gradually diminishes in strength, we omitted the solid line.

DISCUSSION

The strong gas reflector underlies an area of about 3 x 16 km, elongated east-west, and located directly west of Narwhal Island along the seaward boundary of Stefansson Sound. A number of test borings in the vicinity (Harding and Lawson Assoc., 1979) show that the anomalous reflector is associated with a change from stiff marine clay-silt-fine sand to an underlying thick accumulation of presumably non-marine sandy gravel or gravelly sand. The stiff silty clay apparently forms a seal, trapping gas in the coarser materials below. The effectiveness of the cap is shown by a lack of gas in surficial sediment collected near test boring 11 by P.W. Barnes (oral communication).

Strong reflectors with characteristically abrupt terminations, similar to the one under investigation here, are widespread on the Beaufort Sea shelf. The previously unexplained phenomenon has led to uncertainties in interpretations and even to misinterpretations of regional shelf stratigraphy. Thus, Reimnitz et al. (1972) mapped the strong anomalous reflector investigated in this study as the base of a section of Holocene marine sediments about 20 m thick. Since then Reimnitz and Ross (1979) have shown that the area mapped here is underlain by gas-rich sediments coincides with areas where the Quaternary Gubic Formation crops out and Holocene sediments are absent.

Judging by the bonuses offered in the recent State/Federal lease sale, the region here mapped as underlain by shallow gas also has high potential for petroleum accumulations at depth. There is evidence for numerous shallow gas

accumulations, still unmapped, in other areas of the Beaufort Sea shelf that are awaiting development. Techniques used in the present study allow for identification of such accumulations by geophysical methods. Good drilling practice will call for precautionary measures where shallow gas accumulations occur.

CONCLUSION

We have applied quantitative digital processing techniques to high-resolution seismic reflection data obtained near Prudhoe Bay, Alaska, to point out the presence of gas in the pore space of seafloor sediments at shallow depth. Analysis of a suite of seismic records from the same area indicates that the gas-bearing layer, at depths of 20-35 m below the mudline, underlies an area of more than 50 km^2 west of Narwhal Island, about 25 km NE of Prudhoe Bay. Similar records from other areas of the shallow shelf in the Beaufort Sea suggest that patches of shallow gas are a widespread phenomenon. We suggest that appropriate attention be given to the potential effects of shallow gas deposits, as they may affect offshore engineering developments.

REFERENCES CITED

Harding-Lawson Assoc., 1979, U.S.G.S. geotechnical investigation Beaufort Sea 1979: avail. from National Geophysical and Solar-Terrestrial Data Center, Boulder, Colo., 3 vol. + supporting documents, Ref. # AK 17718.

Hunter, J. A., Neave, K. G., MacAulay, H. A., and Hobson, G. D., (1978), Interpretation of sub-seabottom permafrost in the Beaufort Sea by seismic methods. Part I. Seismic refraction methods, in National Research Council of Canada: Proceedings of the third international conference on permafrost, 1978, vol. 1, p. 514-520.

Rogers, J. C., and Morack, J. L. (1978) Geophysical investigation of offshore permafrost, Prudhoe Bay, Alaska, Interpretation of sub-seabottom permafrost in the Beaufort Sea by seismic methods. Part I. Seismic refraction methods, in National Research Council of Canada: Proceedings of the third international conference on permafrost, 1978, p. 560-566.

Reimnitz, Erk and Robin Ross, 1979, Lag deposits of boulders in Stefansson Sound, Beaufort Sea Alaska: U.S. Geological Survey Open File Report 79-1205, 26 p.

Reimnitz, E., Wolf, S. C. and Rodeick, C. A. 1972, Preliminary interpretation of seismic profiles in the Prudhoe Bay area, Beaufort Sea, Alaska. U.S. Geological Survey open file report 548, 11 pp.

Figure 1. Zero-phase wavelet deconvolution is applied to the seismic trace to convert the seismic source pulse to an approximately spike-like form, which permits maximum spatial resolution and unabiguous measurements of amplitude and polarity. A. Typical isolated seismic source pulse, representing the physical characteristics of the seismic source, as modified by transmission through water, and filtering by the hydrophone array, bandpass filters, and the recording and playback systems. The energy is spread out in time over a number of peaks and troughs of the waveform. B. Zero-phase wavelet deconvolution of the source pulse in A., illustrating the symmetry of the zero-phase reconstruction and the small width resulting from inverse filtering, which equalizes spectral energy over a broad range of frequency. The sense, or polarity, of the deconvolved pulse is unabiguous. The arrival of the maximum energy of the pulse occurs at the beginning of the waveform, rather than at a later time as in the case of the original pulse in A. The deconvolved pulse is not a perfect spike (delta-function) because the bandwidth of the deconvolved pulse, though broad, is limited by the frequency range of good signal-to-noise ratio. The isolated pulse shown here represents a single seismic reflector; the actual seismic trace consists of a train of pulses, each produced by a reflecting interface.

Figure 2. Section of shipboard seismic record, in which the reflector identified in this study as gas can be clearly seen. The portion of the record within the box is that subjected to detailed digital analysis in fig. 4. The segment of the gas reflector within the box includes a termination of the reflector on the left end. The water-column multiples of the seafloor (SFM), and the gas reflector (GRM) can be seen about 13 msec below the primary reflections.

Figure 3. Replot, from magnetic tape, of the same data as in fig. 2, performed in the laboratory by a real-time seismic processing system, showing the seafloor and the gas reflectors, with their water-column multiples, more clearly than in the poor quality unprocessed shipboard shown in fig. 2. The portion of record treated in fig. 4 is outlined.

Figure 4. Deconvolved data from the area outlined in figures 2 and 3. A. Clipped wiggle-trace presentation, corresponding to a normal seismic section, showing only the positive portion of the waveform. B. Same data, but subjected to 5-fold vertical stacking, without clipping, showing positive and negative sides of the wave form, in order to emphasize the negative polarity of the gas reflector. These sections are reversed left to right, compared to figures 2 and 3.

Figure 5. Large-scale wiggle-trace presentation of the same data as in figure 4, but subjected to 20-fold vertical stacking. Zero-phase wavelet deconvolution was performed before stacking. The large-amplitude negative spike (opposite in sense to the seafloor reflection event) representing the gas reflector shows the negative polarity and strength of this reflector. Each trace is normalized to the largest amplitude on the trace. The direct arrival followed by its reflection from the hull of boat can be seen ahead of the seafloor reflection. Under 20-fold stacking, the gas reflector is somewhat degraded in amplitude because the reflector is somewhat curved, particularly on the western-most trace. Traces are corrected for spherical spreading.

Figure 6. Magnified view of the gas reflector shown in figure 4, presented at two levels of sensitivity. A. Trace clipped at one-tenth of maximum amplitude, with threshhold at zero amplitude, to emphasize weakest events. B. Trace clipped at 4-tenths maximum aplitude, with threshhold at 0.1 of the clipping amplitude, showing stronger events. The possible lower boundary of the gas-charged zone is indicated, along with the apparent pinch-out near the center of the picture. The layer may not in fact pinch out completely, but may instead become too thin to be resolved with the range of signal frequencies used (less than 2000 Hz).

Figure 7. Conventional seismic records, selected from nearby tracklines shot in prior years, showing characteristic variations of the gas reflector over extended distances. In general the terminations and variations in strength of the gas reflector are unexplained, but may be due to changes in the overlying sedimentary section or to changes in the reflector itself.

Figure 8. Seismic trackline coverage showing the extent of the gas reflector in Stefansson Sound. The reflector was first identified by seismic signal analysis and then mapped by comparing the section of analyzed record with conventional records from the area. The indicated reflector depths below the mudline in meters (small numbers within the gas area) are based on reflection time, assuming an average velocity of 2000 m/sec in the subbottom. The location of the digital seismic analysis of figure 4 is within the dot representing drill hole 11. The 5-meter isobath is shown.

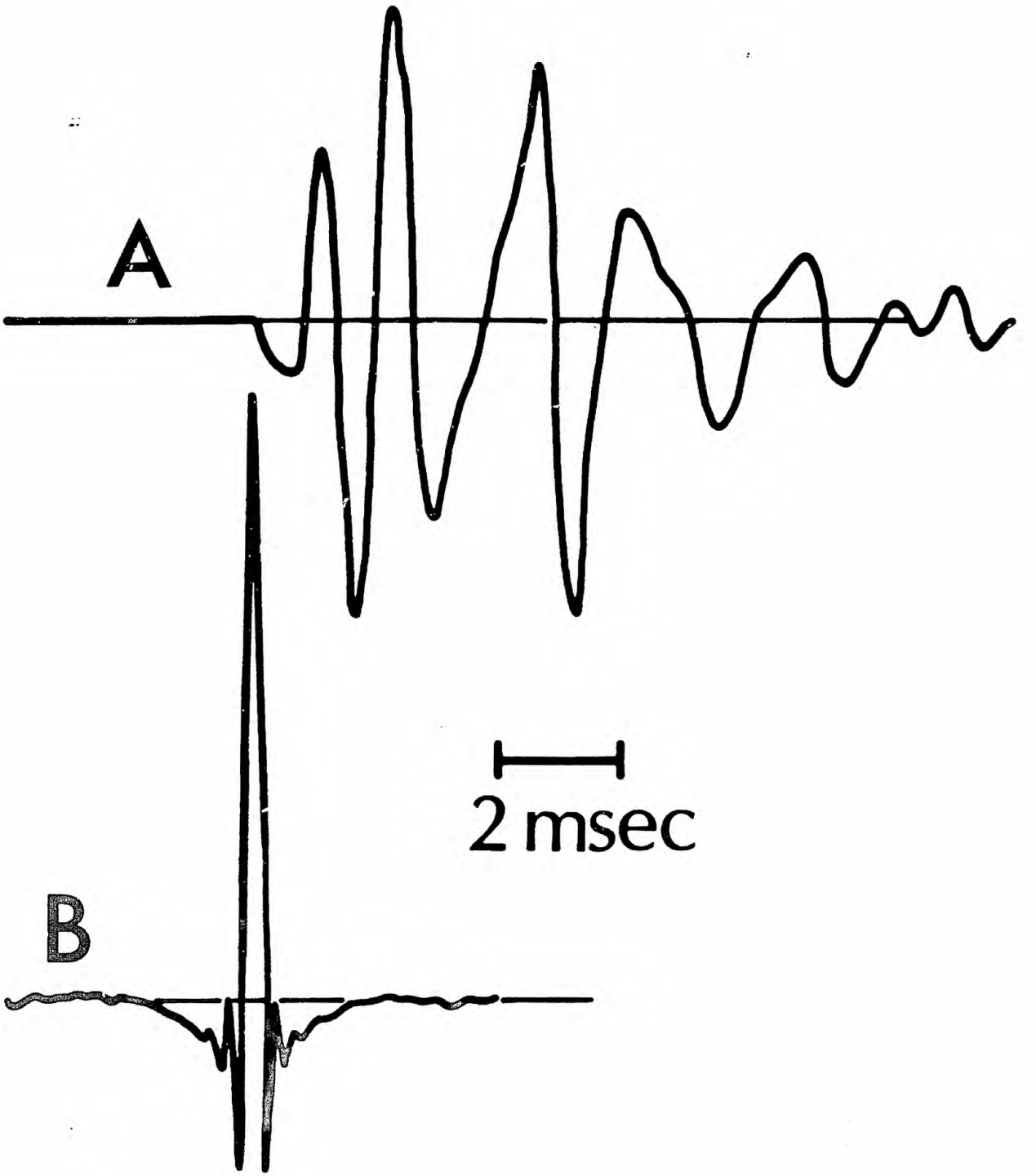

1

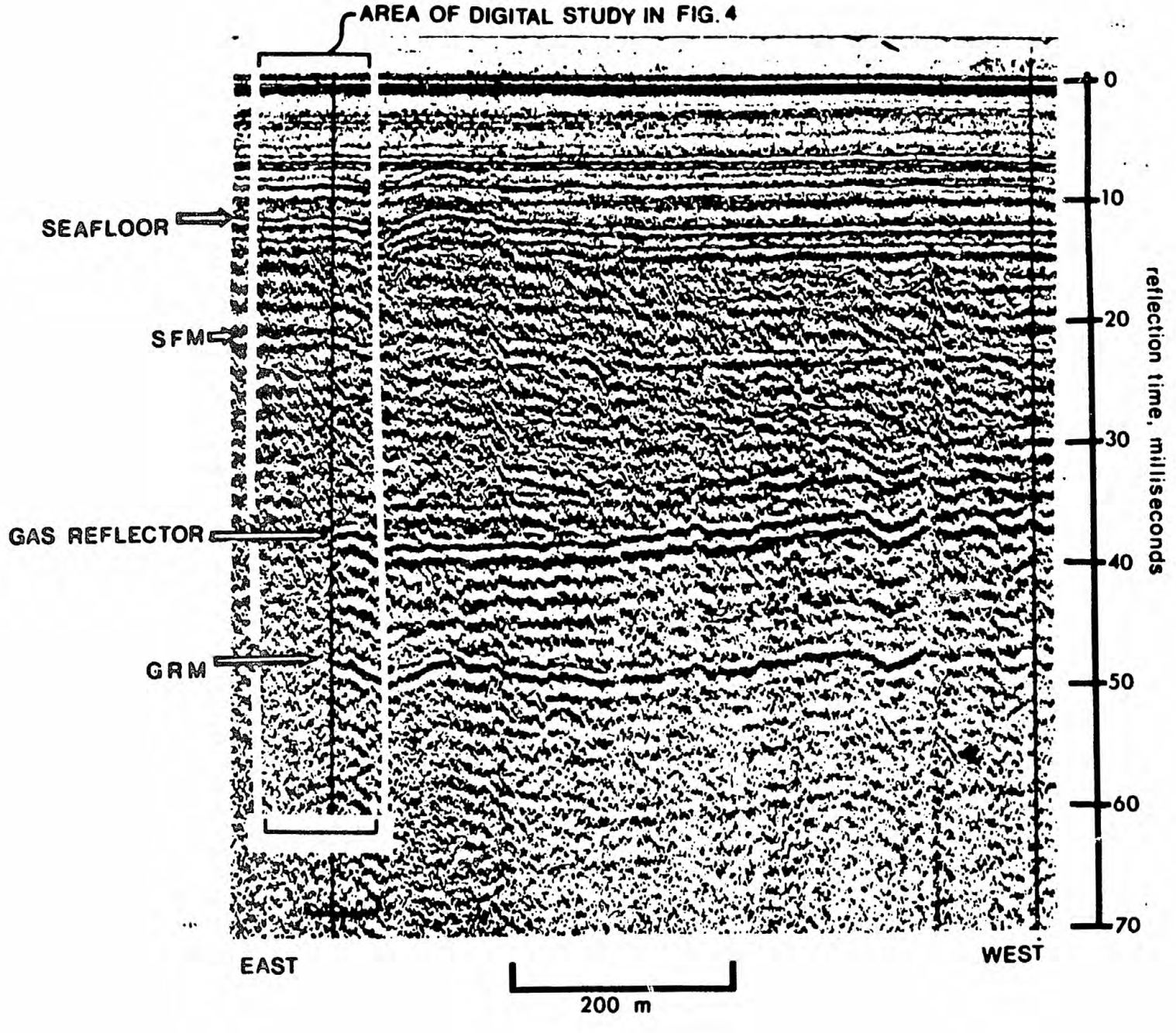
AREA OF DIGITAL STUDY IN FIG. 4
SEAFLOOR
SFM
GAS REFLECTOR
GRM
EAST
WEST
200 m
0
10
20
30
40
50
60
70
reflection time, milliseconds

2

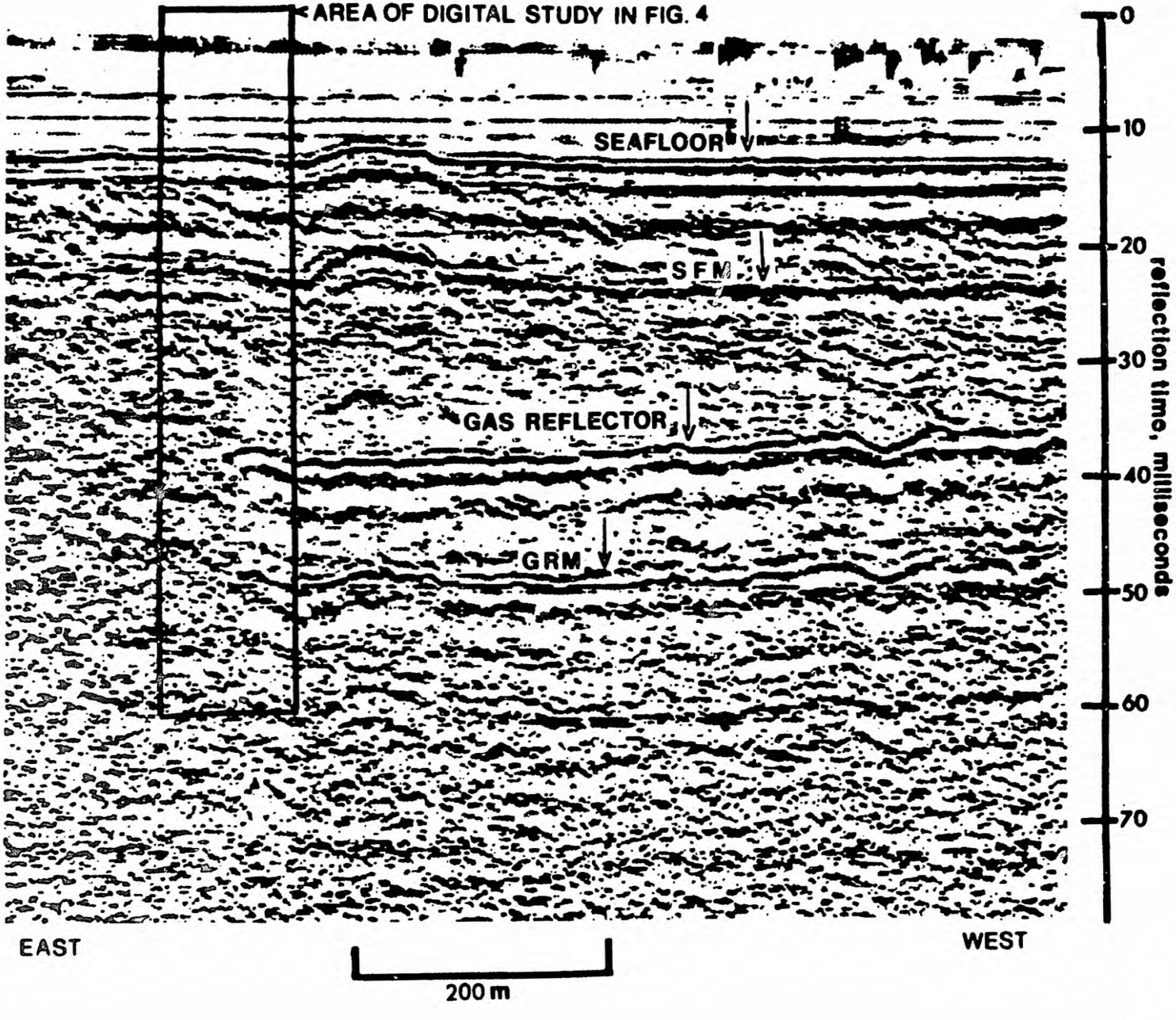
AREA OF DIGITAL STUDY IN FIG. 4
SEAFLOOR
SFM
GAS REFLECTOR
GRM
0
10
20
30
40
50
60
70
reflection time, milliseconds
EAST
WEST
200 m

3

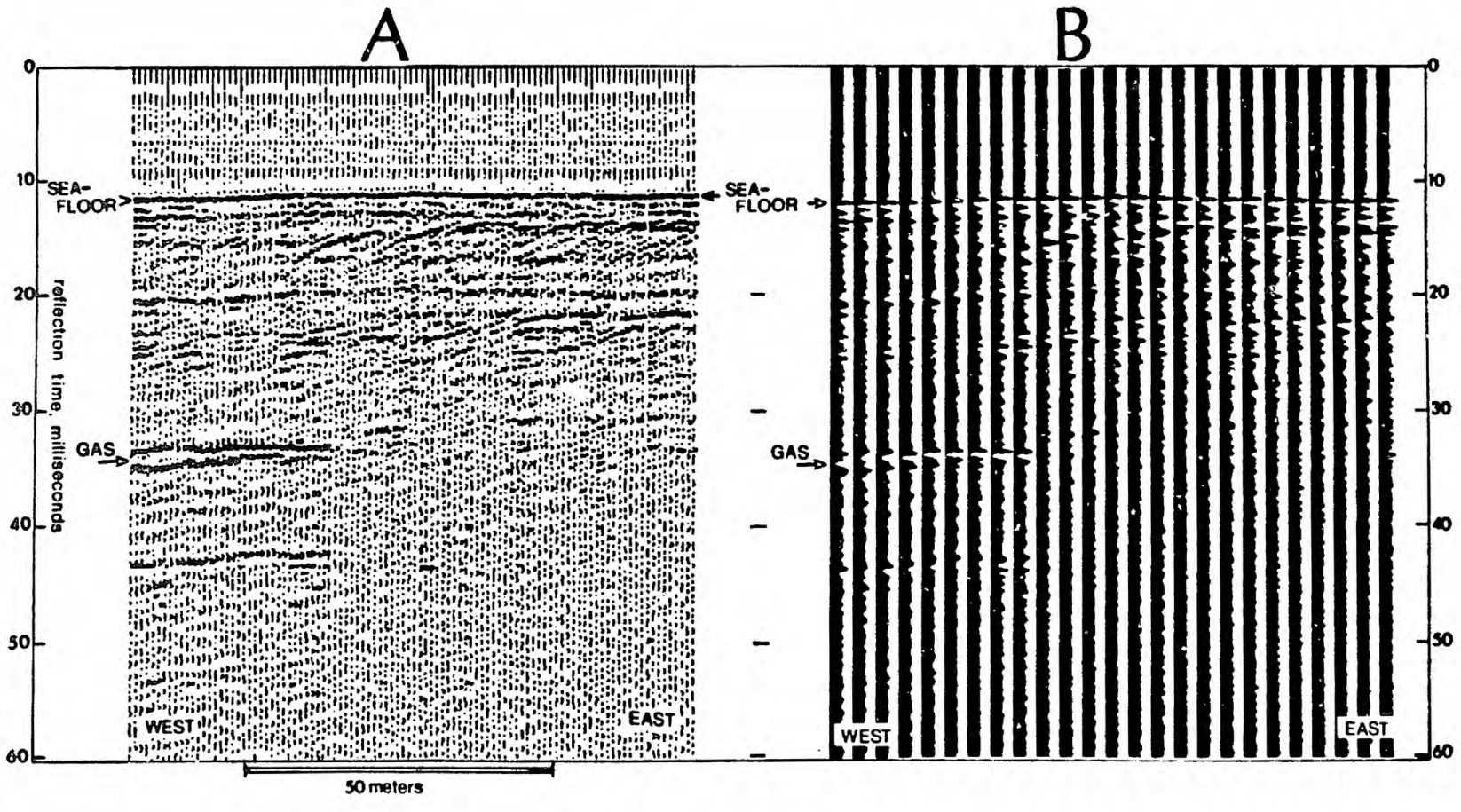
A
B
0
10
20
30
40
50
60
SEA-
FLOOR
GAS
reflection time, milliseconds
WEST
EAST
50 meters

4

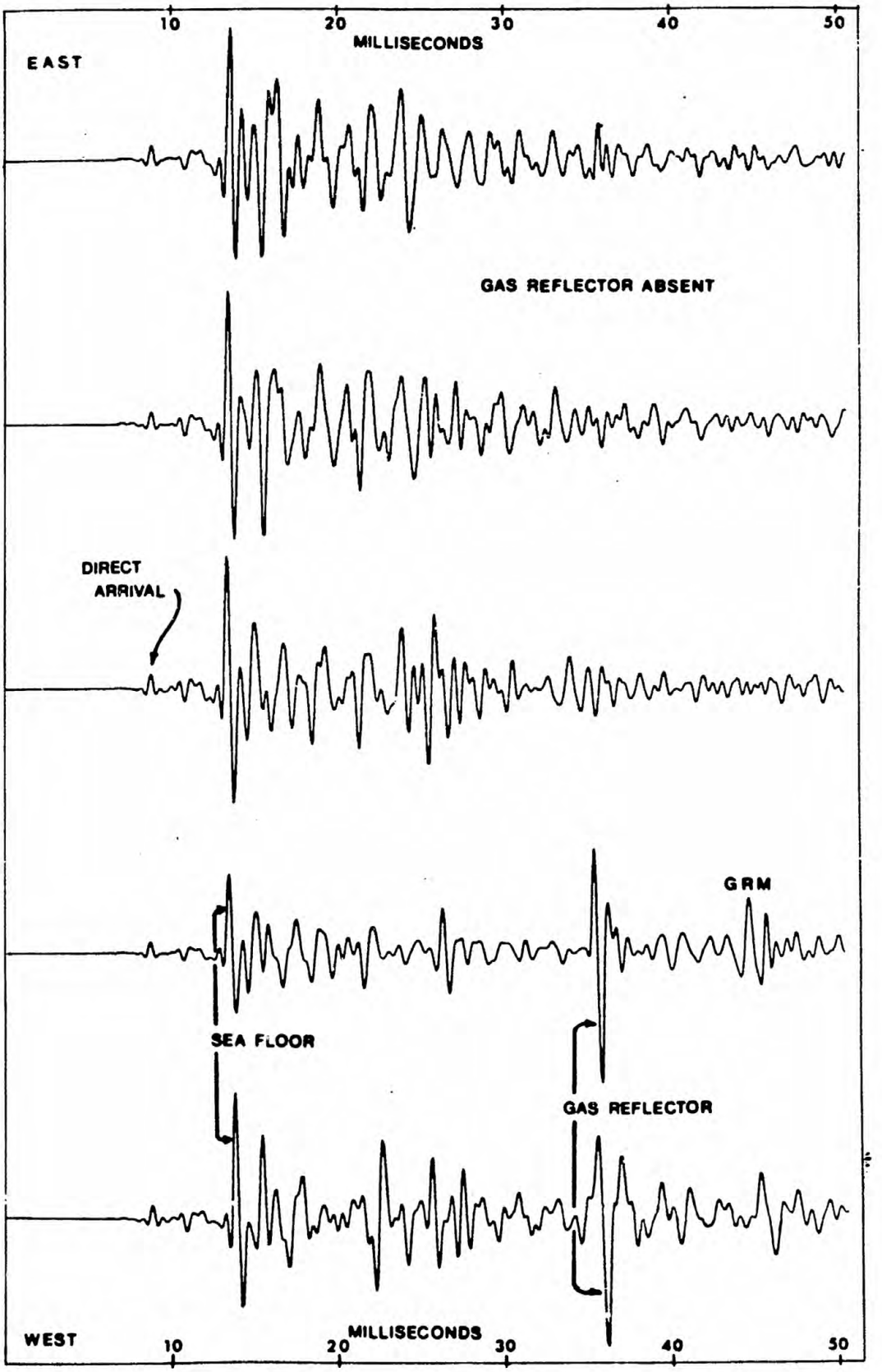
10
20
30
40
50
MILLISECONDS
EAST
GAS REFLECTOR ABSENT
DIRECT
ARRIVAL
GRM
SEA FLOOR
GAS REFLECTOR
WEST
10
20
MILLISECONDS
30
40
50

5

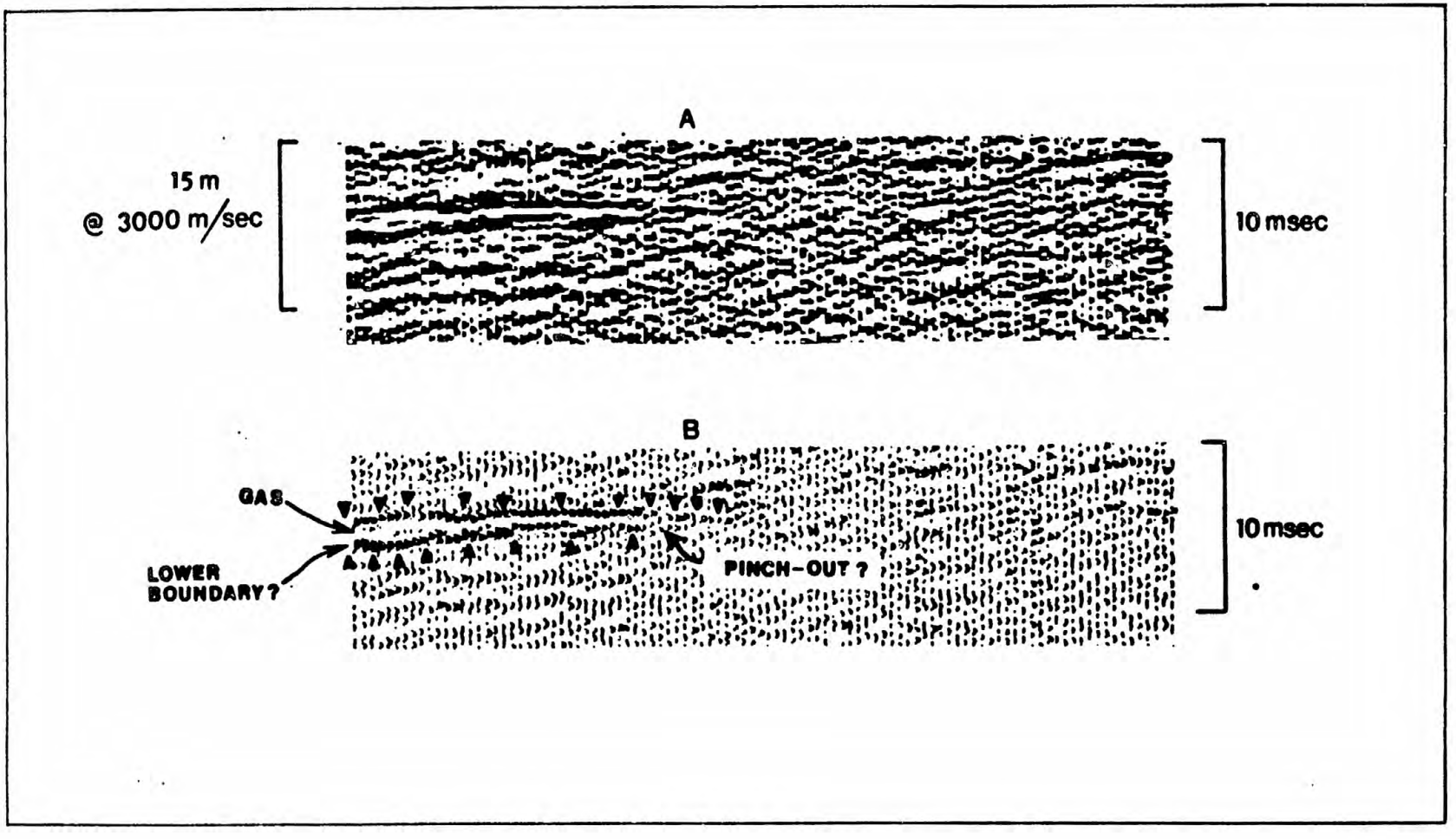
A
15 m
@ 3000 m/sec
10 msec
B
GAS
LOWER
BOUNDARY?
PINCH-OUT ?
10 msec

SEAFLOOR
GAS LAYER
0.1 SECOND
500 m
SEAFLOOR
GAS LAYER
MULTIPLE REFLECTIONS
0.1 SECOND
500 m

7

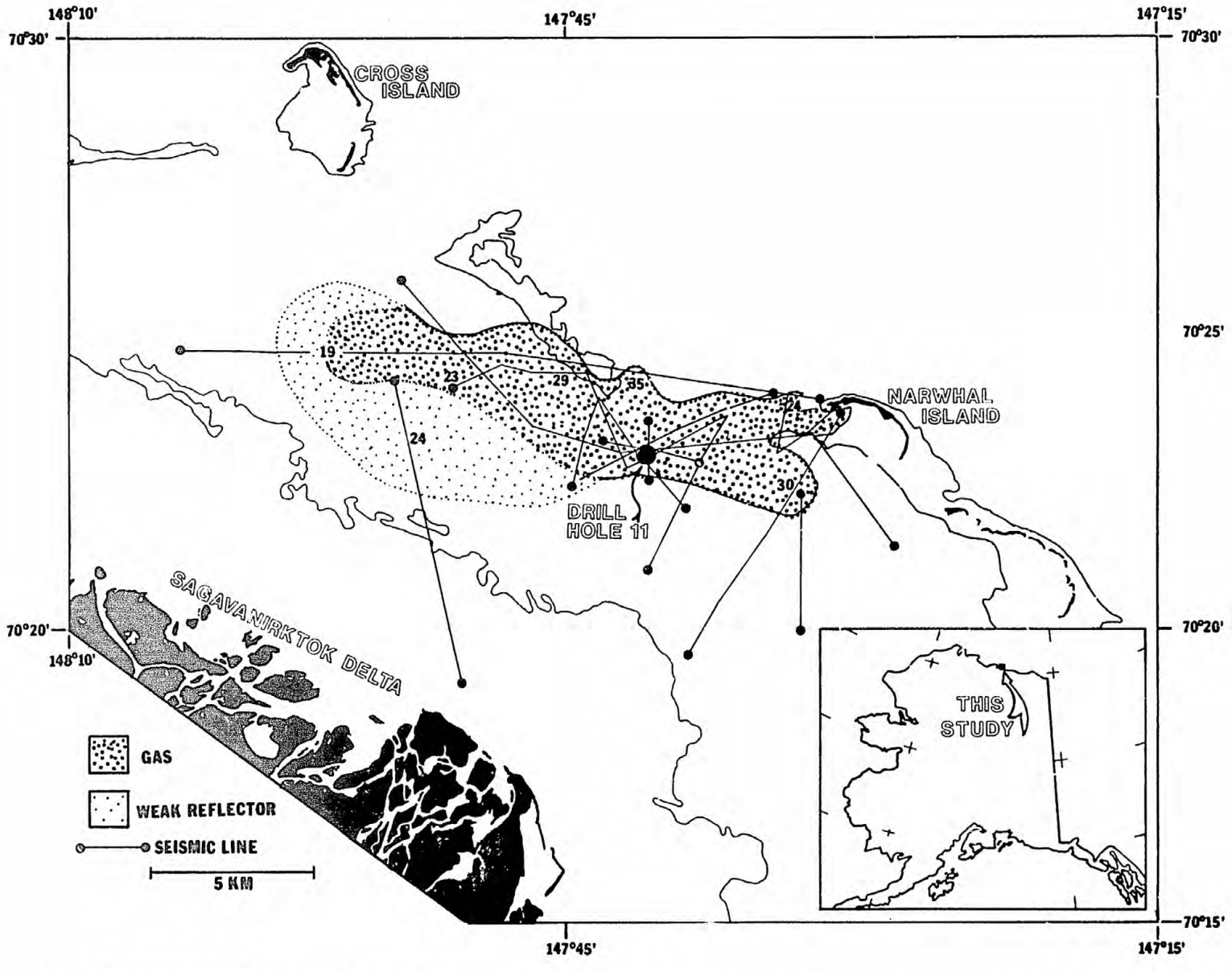
148°10'
147°45'
147°15'
70°30'
70°25'
70°20'
70°15'
CROSS ISLAND
NARWHAL ISLAND
DRILL HOLE 11
SAGAVANIRKTOK DELTA
19
23
29
35
24
24
30
THIS STUDY
GAS
WEAK REFLECTOR
SEISMIC LINE
5 KM